Materials Science and Technology

ISSN: 0267-0836 (Print) 1743-2847 (Online) Journal homepage: https://www.tandfonline.com/loi/ymst20

Effect of Mn on cooling behaviour and microstructure of chill cast Zn–Al (ZA8) alloy

G Ramesh, H M Vishwanath & K N Prabhu

To cite this article: G Ramesh, H M Vishwanath & K N Prabhu (2012) Effect of Mn on cooling behaviour and microstructure of chill cast Zn–Al (ZA8) alloy, Materials Science and Technology, 28:11, 1301-1307, DOI: 10.1179/1743284712Y.0000000057

To link to this article: https://doi.org/10.1179/1743284712Y.0000000057

Effect of Mn on cooling behaviour and microstructure of chill cast Zn–Al (ZA8) alloy

G. Ramesh, H. M. Vishwanath and K. N. Prabhu*

In the present work, the effect of manganese addition to ZA8 alloy on thermal analysis parameters, heat transfer and microstructure was investigated. The thermal analysis parameters were found to be significantly affected by chemical modification of ZA8 alloy. Cooling curve and differential scanning calorimetry analyses of modified alloy showed nucleation of new phase other than β dendrites. Chilling of modified alloy resulted in decreased liquidus temperature and enhanced eutectoid transformation. Further, chilling avoids the formation of intermetallic compounds in modified alloy. The heat flux transients were estimated using inverse modelling during solidification of unmodified and modified alloys against different chills. The peak heat flux decreased on addition of Mn to ZA8 alloy. Differential scanning calorimetry analysis indicated that the addition of Mn to ZA8 alloy decreases the heat of solidification. The addition of Mn to ZA8 alloy increased the contact angle, indicating decreased wettability of the modified alloy on the chill surface. The microstructure of ZA8 with Mn showed an increased amount of β phase and a decreased amount of eutectic. X-ray diffraction analysis confirmed the formation of $MnAl_6$ intermetallics in Mn added ZA8 alloy. Chilling with chemical modification resulted in enhanced decomposition of β phase.

Keywords: Zn–Al (ZA8) alloy, Manganese modification, Thermal analysis, Microstructure

Introduction

Zinc aluminium die cast alloys are used in a variety of applications because of their higher strength and hardness, improved wear resistance and creep resistance and lower densities. Zinc aluminium casting alloys are mainly classified into two groups, namely, ZAMAK and ZA alloys. ZAMAK alloys have 4% aluminium as the primary alloying constituent with less amount of magnesium, and these alloys are identified as nos. 3, 5, 7 and 2. ZA alloys have a higher amount of aluminium and copper, and these alloys are identified as ZA8, ZA12 and ZA27, in which the number represents the percentage of aluminium in the alloy.[1–3] The mechanical properties of zinc aluminium alloys mainly depend on the presence and amount of varying alloying elements and the final microstructure of casting. The microstructure of the casting can be modified by: additions of alloy modifiers, varying the cooling conditions during solidification and heat treatment of casting. Yan *et al.* investigated the effect of the addition of Mn, RE, Ti and B on the microstructure and tribological behaviour of ZA27 alloy. The unmodified alloy was characterised by α (Al rich solid solution) dendrite with some $(\alpha+\beta)+(\alpha+\beta+\varepsilon)$ eutectics and ε phases dispersed in the interdendrite region. The modified alloy shows more hard intermetallics such as Al_5MnZn, $Al_9(MnZn)_2$ and $Al_{65}Mn(RE)_6Ti_4Zn_{36}$ dispersed in the eutectic region and α dendrites. The grain size of α phase of modified alloy is finer than ZA27 alloy. Further, elevated temperature strength, antifriction and wear resistance of modified alloys were better compared to ZA27.[4] They also observed that the increase in Mn content from 0·18 to 1·22 results in an increase in size and volume fraction of intermetallic compounds, and the morphology of intermetallic compounds changes gradually from fine particulates to coarse rod shape.[5] Similarly, Dominguez *et al.* studied three different shapes of Al–Mn precipitates (i.e. globular, plate-like and faceted) in ZA27 alloy by Mn addition.[6] Zhu *et al.* observed that the copper modified ZA8 alloy consists of a tree stem shaped eutectic structure together with flower-like cores of solidification, which were surrounded by a large amount of eutectoid structure. Further aging at 150°C results in two stages of phase transformation, i.e. decomposition of zinc rich η phase and four-phase transformation $\alpha+\varepsilon\rightarrow T'+\eta$.[7] Prasad studied the heat treatment of zinc aluminium alloy containing nickel and observed uniformly distributed microconstituents in the alloy without affecting the morphology of the nickel containing microconstituents. He obtained improved wear resistance even though heat treatment of the alloy reduced the hardness.[8] Savaskan and Bican have reported that the wear resistance, hardness and tensile strength of the Zn–Al–Cu alloy increase by addition of up to 2·5%Si and decreases thereafter.[9] Turk *et al.* studied the addition of

Department of Metallurgical and Materials Engineering, National Institute of Technology Karnataka, Srinivasnagar, Mangalore 575025, India

*Corresponding author, email prabhukn_2002@yahoo.co.in

Published by Maney on behalf of the Institute
Received 14 April 2012; accepted 24 April 2012
DOI 10.1179/1743284712Y.0000000057

Mn in the range 0·01–0·53 wt-% on the microstructure and mechanical properties of ZA8 alloy. The addition of Mn modifies the as cast microstructure by reducing the size of β dendrites and increasing the amount of eutectic phase in a more regular form and also forms a small, fine and irregularly shaped intermetallic compound ($MnAl_6$) in the dendrites and eutectic regions. The number and size of intermetallic particles increase with manganese content. The hardness and creep strength of the ZA8 alloy increased with increasing manganese content, whereas 0·2% yield, tensile and impact strengths of the alloy improved with increasing Mn up to 0·045 wt-% and then reduced gradually with a further increase in manganese. Optimum mechanical properties were achieved by the addition of 0·045–0·063 wt-%Mn.[10] Seenappa and Sharma observed hard intermetallic compounds such as $CuZn_5$, $CuAl_2O_4$, Al_4Cu_9 and Al_4Cu_3Zn during solidification of Zn–Al25 with the addition of copper. The tensile strength, yield strength and ductility of the alloy increased continuously with increasing copper content, while the impact strength decreased after 2 wt-% copper.[11] Krupinska *et al.* investigated the effect of cooling rate on the microstructure of Zn–Al casting. The increase in cooling rate from 0·08 to 0·68°C s^{-1} results in refinement of the microstructure as well as increase in the alloy hardness ~24·9%.[12] They also investigated the effect of addition of La and Ce into the ZnAl8Cu1 alloy. The addition of La and Ce causes only refinement of grains and subgrains in the microstructure but no occurrence of new phases or eutectics during the crystallisation process of the alloy.[13] Mojaver and Shahverdi found that the grain size, secondary dendrite arm spacing, density of ε precipitates and amount of eutectoid $\alpha+\eta$ increased with decreasing cooling rates of Zn–27%Al alloys containing >2%Cu.[14]

The advantage of ZA8 is that it can be hot chamber die cast, and its strength and hardness are significantly higher than those of no. 3 alloy. Preliminary creep evaluations suggest that design stress levels for ZA8 die castings can be three times higher than those for ZAMAK at room temperature.[15] The addition of Mn to ZA8 alloy improves its creep resistance especially at temperatures >100°C.[10] Further, in die casting applications, the alloy is subjected to intense chilling. It is interesting to assess the combined action of chilling and Mn modification on heat transfer and evolution of microstructure. Previous studies on Al–Si alloys have shown that Na/Sr modification and chilling have significant effect on the cooling behaviour of the alloy, heat transfer and microstructure. Computer aided cooling curve analysis is a useful tool for the non-destructive assessment of melt quality and is extensively used in the assessment of modification of Al–Si alloys. The determination of metal/mould heat flux transient is essential for the simulation of solidification of castings. In the present work, the effect of addition of Mn on thermal analysis parameters, metal/chill interfacial heat transfer and microstructure of ZA8 alloy was investigated.

Experimental

Commercially pure ZA8 alloy ingots were used for the solidification experiment. The composition of the ZA8 alloy is given in Table 1. The alloy ingots were cut into small pieces weighing ~1300 g. A calculated amount of manganese flakes (0·5 wt-% of ZA8 alloy) is well ground in a porcelain mortar and pestle. The powdered Mn along with pieces of ZA8 alloy is taken in a graphite crucible and melted to 675°C in an electric resistance furnace. The alloy melt was stirred for 5 min using graphite rod and then transferred to preheated no A-1 graphite crucible. The melt is placed back in the furnace and maintained at a constant temperature of 600°C for 15 min.

Aluminium, copper, hot die steel (HDS) and stainless steel (SS) having varying thermal conductivities were used in the present study for chilling of the liquid metal. These chills give different cooling rates during solidification. Each chill is of 100 mm length and 25 mm diameter. Two holes of diameter 1 mm were drilled on the cylindrical surface of the chills at distances 2 and 14 mm from the casting/chill interface to accommodate thermocouples.

Two types of thermocouples were used at three different locations. Two mineral insulated and sheathed SS K type thermocouples of diameter 1 mm were inserted on the chill. Another K type thermocouple prepared in the laboratory by joining chromel–alumel wires of 0·45 mm diameter, which was inserted in twin bored ceramic beads of 5 mm diameter, was placed in the liquid melt to measure the casting temperature during solidification. All thermocouples were connected to a data acquisition system NI PXI/PCI-4351 using compensating cables.

In thermal analysis, the temperature of the solidifying metal is monitored and recorded. The crucible containing the molten alloy is quickly transferred to the insulated base of the experimental set-up. The instrumented chill was lowered into the crucible such that its bottom surface just comes into contact with the liquid melt. Figure 1 shows the schematic sketch of the experimental set-up. Temperature data from both casting and chill were recorded at 0·3 s interval using a computerised data acquisition system.

The heat flux at the surface of the chill was estimated from the measured temperature history and thermophysical properties of the chill material using inverse method. The equation that governs the two-dimensional transient heat conduction in cylindrical coordinates is given below

$$\frac{1}{r}\frac{\partial}{\partial x}\left(rk\frac{\partial T}{\partial r}\right)+\frac{\partial}{\partial z}\left(k\frac{\partial T}{\partial z}\right)=\rho C_{\mathrm{p}}\frac{\partial T}{\partial t}$$

The above equation was solved inversely using SOLVERinverse (TherMet Solutions Pvt. Ltd, Bangalore) software for the estimation of heat flux transients.

Contact angle measurements were carried out on solidified droplets of both modified and unmodified ZA8 alloys. Unmodified and modified ZA8 alloys weighing ~2 g were placed on copper plates polished using 180 grit silicon carbide paper. The plates were heated in an electric furnace to melt the alloy and then allowed to cool so that the liquid melts solidify. The contact angles were measured using FTA200 (First Ten Angstroms) contact angle analyser.

Table 1 Chemical composition of ZA8 alloy/wt-%

Al	Mg	Cu	Fe	Pb	Cd	Sn	Zn
8·2–8·8	0·02–0·03	0·9–1·3	0·035	0·005	0·005	0·002	Balance

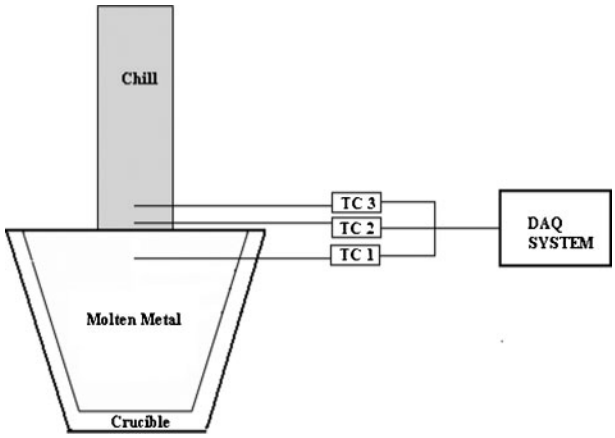

1 Schematic sketch of experimental set-up

X-ray diffraction (XRD) study was carried out using a JEOL JDX-8P-XRD system. Samples having 5×5 mm size were made for both unmodified and modified ZA8 alloys. The surface on which the XRD analysis was to be carried out was ground and polished using SiC paper. The samples were placed in an aluminium plate holder, and diffraction study was conducted at a scan speed of 2° min^{-1} in a step size of 0·02. The XRD pattern was generated and analysed to assess the possibility of formation of intermetallics.

Differential scanning calorimetry (DSC) analysis of modified and unmodified ZA8 was carried out on a DSC analyser. About 4·7 mg of modified ZA8 alloy was placed on silver pans, which were kept on the melting table of the equipment. The operating temperature was 550°C. The temperature of the system was gradually raised from room temperature to 550°C at a rate of 10° min^{-1}. A plot of heat energy versus temperature was obtained and analysed for the determination of the nature of the reaction involved during melting. The same procedure was repeated for the unmodified ZA8 alloy also.

The specimens for metallographic study were prepared from sections of castings taken at ~1 cm from the casting/chill interface. The specimens were then ground successively on 180, 220, 400, 600, 800 and 1200 grit silicon carbide papers. Each specimen was washed and dried thoroughly after each cycle of polishing. The final polishing was performed using a rotating disc polisher with 0·3 μm levitated alumina. The specimens were washed and dried thoroughly and etched using concentrated HCl for ~1–2 s. The microstructures of each specimen were then examined using a JEOL JSM 6380LA scanning electron microscope (SEM) with energy dispersive spectroscopy facility.

Results and discussion

Figure 2 represents the cooling behaviour of ZA8 alloys unmodified and modified with Mn solidified in a fireclay crucible subjected to furnace cooling. It shows three temperature arrests, namely, liquidus temperature T_{liquidus}, eutectic start temperature T_{eutectic} and eutectoid temperature $T_{\text{eutectoid}}$. The addition of Mn results in an increase in liquidus temperature and decreases in eutectic and eutectoid temperatures. Further, the time required for cooling from liquidus to start of eutectic (dendritic growth region) was found to be longer. The eutectic arrest time was significantly less compared to the unmodified alloy. Figure 3 shows the first derivative of the cooling curve of the unmodified and modified ZA8 alloys. Three valleys in the cooling curve were observed (designated as p, q and r) and correspond to regions of nucleation of β dendrites, eutectic transformation and eutectoid transformation respectively. The cooling rate curve of modified alloy shows two valleys in the nucleation region, indicating the nucleation of another new phase. Further, in the eutectic transformation region, the valley shows the loop behaviour that indicates the occurrence of undercooling. The magnified regions of liquidus temperature and eutectic start temperature of the modified alloy (Fig. 2*b*, inside) clearly show short liquidus arrest of ~31 s and small degree of undercooling of ~0·12°C at the eutectic. Differential scanning calorimetry analyses of the unmodified and modified alloys are shown in Fig. 4. The unmodified alloy shows two negative peaks that correspond to eutectic and eutectoid transformations respectively, whereas the modified alloy shows an additional negative peak before eutectic transformation. It clearly confirms the nucleation of a new phase other than β. The binary phase diagrams of Al–Mn and Zn–Mn show the maximum solubility of Mn in Al and Zn is 1·25 wt-% at 656°C and 0·5 wt-% at 416°C respectively.[16,17] Since Mn and Al are cubic structures (whereas Zn is HCP), it is expected that the formation of Al–Mn

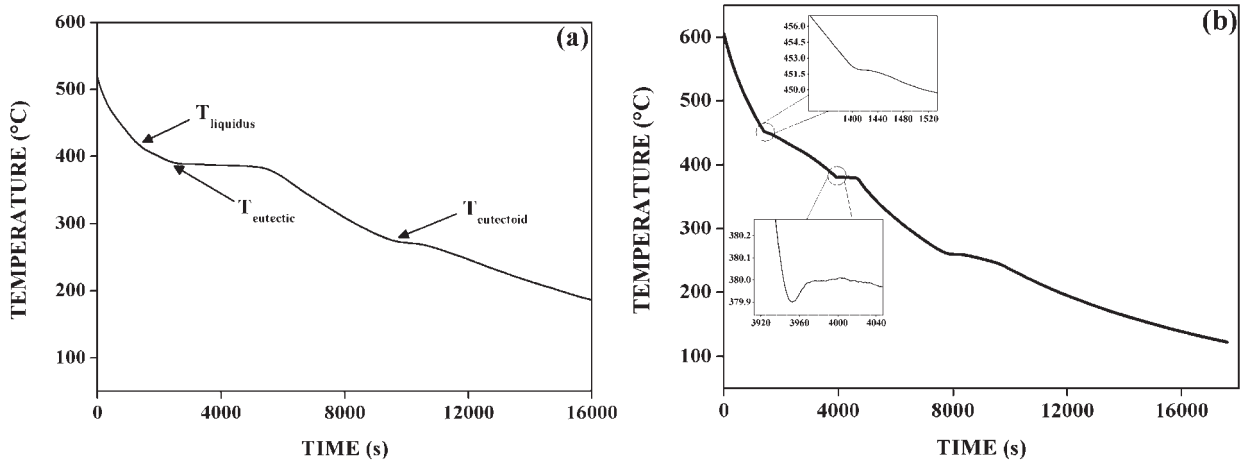

2 Cooling curve of ZA8 alloy *a* unmodified and *b* modified with Mn solidified in crucible

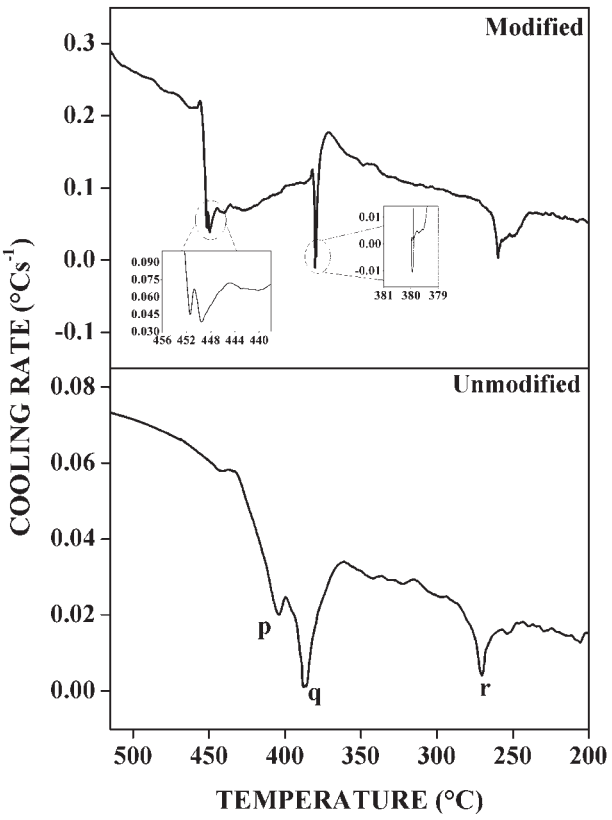

3 Cooling rate curve of unmodified and modified ZA8 alloys solidified in crucible

base crystal nucleates first at higher temperature. Further, it may act as heterogeneous nuclei for β phase. Thus, the liquidus temperature of the modified ZA8 alloy occurs at a higher temperature, and the time required to cool from the liquidus temperature to start of eutectic is also longer compared to the unmodified alloy. Table 2 shows the thermal analysis parameters measured from the cooling curves of the castings. The effect of chilling on the cooling behaviour of the casting is shown in Fig. 5. The supercooling of the casting by chilling during solidification results in decreases in durations of dendrite growth, eutectic and eutectoid transformations. Chilling of unmodified alloy did not show any significant effect on the liquidus and eutectic temperatures of the casting. The cooling curve of the unmodified solidified against chill did not show eutectoid arrest, but the cooling rate of the casting showed valley for eutectoid transformation, which occurs at higher temperature. The possible reason could be that the β phase formed in the short interval during chilling may not be stable and starts to decompose at higher temperature. The cooling curve of the modified alloy solidified against chill shows a different behaviour. It is observed that the liquidus temperature of the modified alloy is significantly reduced by chilling, and the duration of dendrite growth is less compared to the eutectic arrest. It indicates that enhanced cooling of the modified alloy would avoid the formation/nucleation of intermetallic occurring at higher temperature, resulting in lower liquidus temperature. Further, eutectoid transformation was clearly observed and was not seen when unmodified casting was solidified against chill.

Figure 6 shows the typical cooling and heating behaviours of the unmodified and modified ZA8 alloys solidified against aluminium chill. It indicates that chill was heated rapidly in the beginning as the liquid metal cools. When the liquid temperature drops to the eutectic arrest temperature, both alloy and chill temperature curves attain plateau up to the solidus temperature of the alloy. Thereafter, both alloy and chill temperature decrease rapidly. The measured temperature readings of the chill at different locations and thermophysical properties of the chill materials were used for the estimation of heat flux transients using the inverse method. The typical estimated heat flux transients for unmodified and modified ZA8 alloys solidified against aluminium chill are shown in Fig. 7. The heat flux shows a maximum shortly after pouring and then drops off rapidly. The initial heat flux value is high due to the good contact at the liquid metal/chill interface. As the casting started solidifying, the contact becomes nonconforming, resulting in a reduction in heat flux at the interface. The modified alloys show a lower heat flux as compared to unmodified alloys. The peak heat flux values were 1810, 1237, 835 and 758 kW m^{-2} for unmodified alloy solidified against copper, aluminium, HDS and SS respectively.[18] The corresponding values for modified alloy were 1537, 1096, 754 and 714 kW m^{-2}. A contact angle analysis study was carried out to know the effect of Mn on the surface tension of ZA8 alloy. Figure 8 shows the image of unmodified and

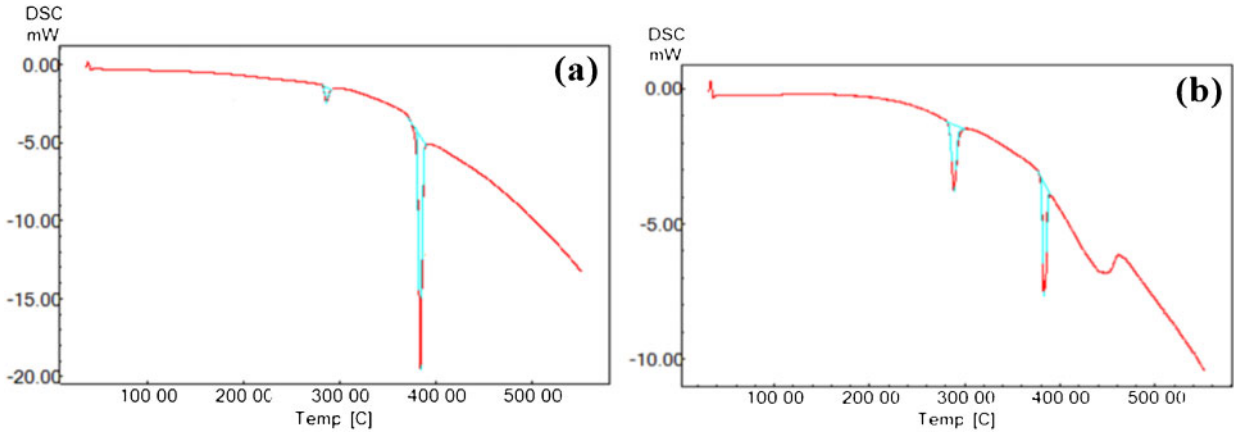

4 Differential scanning calorimetry curve of *a* unmodified and *b* modified ZA8 alloy scanned at heating rate of 10°C min^{-1}

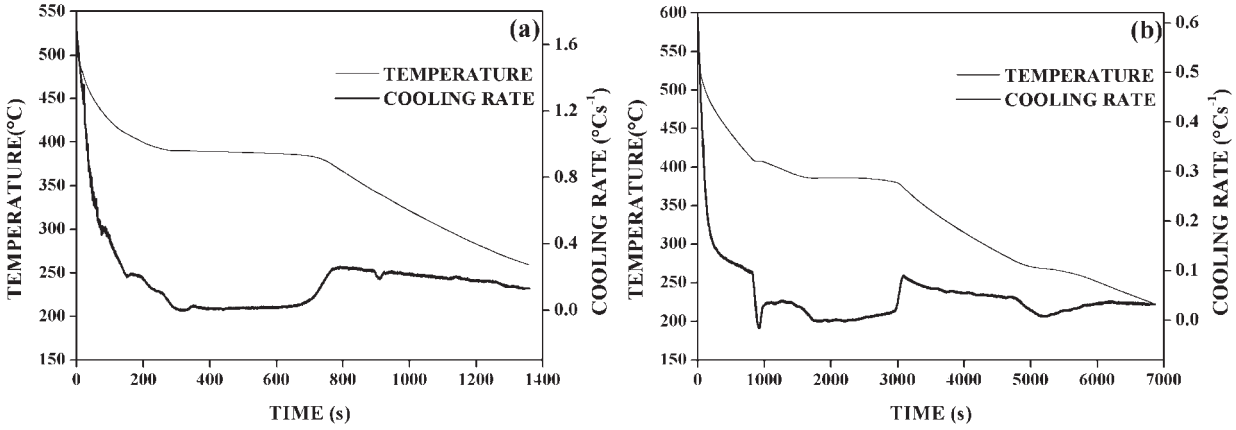

5 Cooling behaviour of ZA8 alloy *a* unmodified and *b* modified with Mn solidified against copper chill

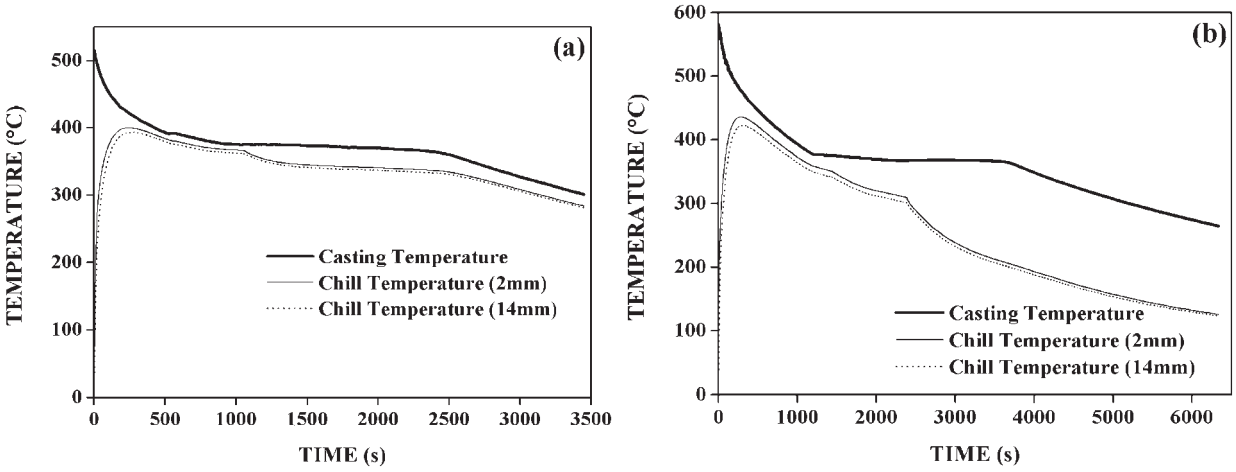

6 Temperature versus time curve of ZA8 alloy *a* unmodified and *b* modified solidified against aluminium chill

modified ZA8 alloy droplets solidified on copper chill. The contact angle for the modified ZA8 alloy droplet was found to be higher than the unmodified ZA8 alloy. Thus, the modified ZA8 alloy has poor wettability. The surface tension of the alloys was estimated from the captured image using Dorsey equation.[19] The surface tension ratio of modified alloy to unmodified alloy was found to be 1·19. It indicates that the addition of Mn to ZA8 alloy increases its surface tension. From the DSC plots, it is observed that the melting of unmodified ZA8 alloy is more endothermic than the modified ZA8 alloy. In other words, the solidification of unmodified is more exothermic than the modified, and hence, modified ZA8 liberates less latent heat during solidification. The increased surface tension and lower latent heat evolved during solidification by the addition of Mn resulted in decreased heat flux transients.

Table 2 Thermal analysis parameters measured using computer aided cooling curve analysis technique

Parameters	Unmodified alloy	Modified alloy
Liquidus temperature/°C	408	452
Eutectic temperature/°C	389	380
Eutectoid temperature/°C	271	260
Liquidus arrest time/s	…	31
Dendrite growth time/s	982	2543
Eutectic arrest time/s	2986	708
Eutectic undercooling/°C	…	0·12

Metallographic studies were carried out to assess the effect of addition of Mn on the microstructure of ZA8 alloy. According to Zn–Al phase diagram, at eutectic temperature, the structure of as cast ZA8 alloy consists of primary β dendrites distributed in a eutectic matrix. On cooling below eutectoid temperature, the β decomposes to α and η phases which are distributed in eutectic matrix. Figures 9 and 10 show the microstructure of the unmodified and modified ZA8 alloys solidified in a

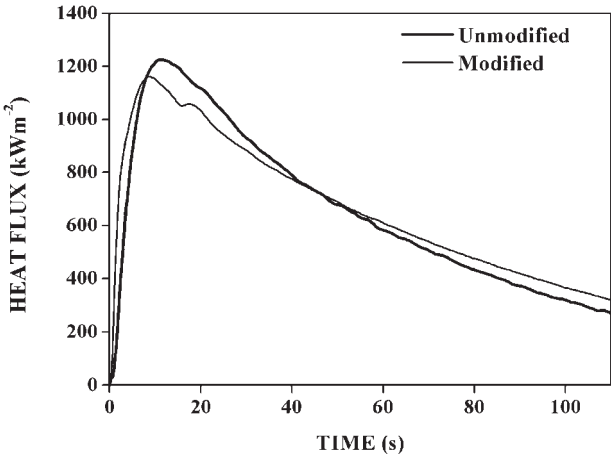

7 Heat flux versus time curve for unmodified and unmodified ZA8 alloys solidified against aluminium chill

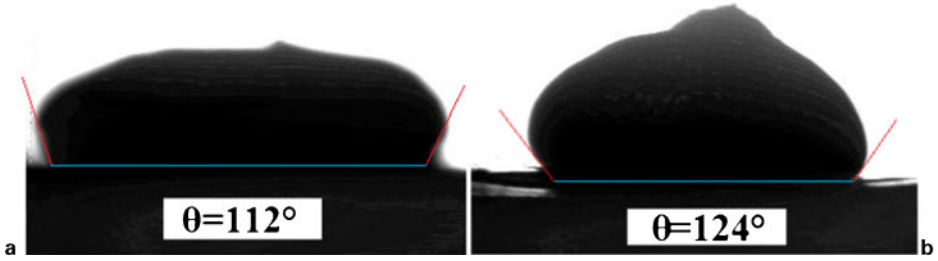

8 Contact angle of *a* unmodified and *b* modified ZA8 alloy droplet on copper substrate

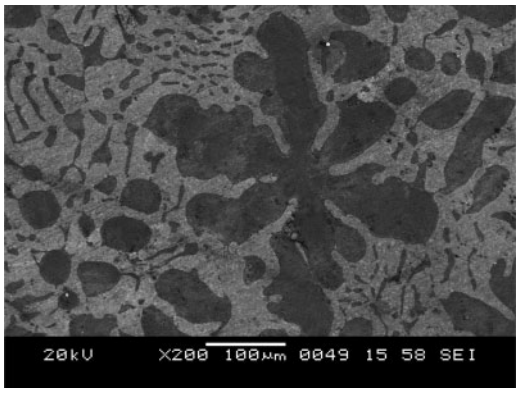

9 Image (SEM) of unmodified ZA8 alloy solidified in fire-clay crucible

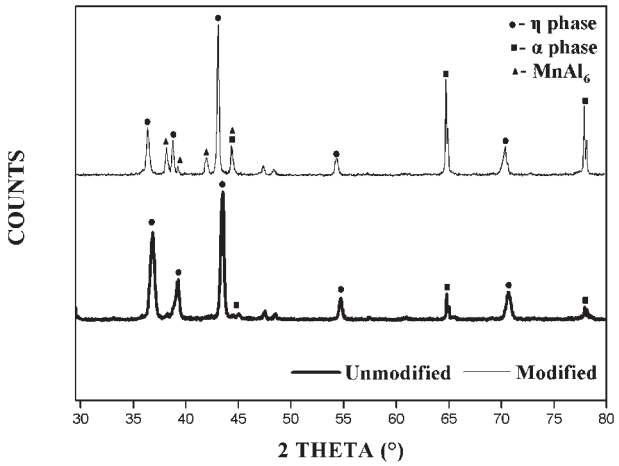

11 X-ray diffraction pattern of unmodified and modified ZA8 alloys

crucible subjected to furnace cooling. The microstructure consisted of primary dendrites in a eutectic matrix. The modified ZA8 alloy shows the presence of irregularly shaped intermetallic compound in the region of both dendrites and eutectic (marked by arrows). The XRD analyses of the unmodified and modified casting samples indicate that the intermetallic compound in the modified ZA8 alloy is $MnAl_6$ (Fig. 11). Further, the modified ZA8 alloy shows increased volume fraction of the dendrite phase and decreased amount of eutectic phase compared to the unmodified ZA8 alloy. Thus, the addition of Mn to the ZA8 alloy results in more nucleation of primary β dendrites. The effect of chilling on the microstructure of the casting is shown in Fig. 12. It is observed that chilling of the casting results in as cast β dendrite morphology transforming to nearly rounded/globular shape and the volume fraction of the eutectic increases. The chilling with chemically modified alloy did not show any presence of intermetallic compound, which confirms that enhanced cooling of the casting by chill avoids the formation of intermetallic. Further, refinement of β phase of Mn modified alloy solidified against chill was observed at higher magnification compared to the unmodified alloy (Fig. 13). The β phase formed in chill cast Mn modified alloy is expected to contain more Mn compared to the eutectic because of the higher solubility of Mn in aluminium than in zinc. Thus, the presence of Mn results in enhancement of the decomposition of the β phase.

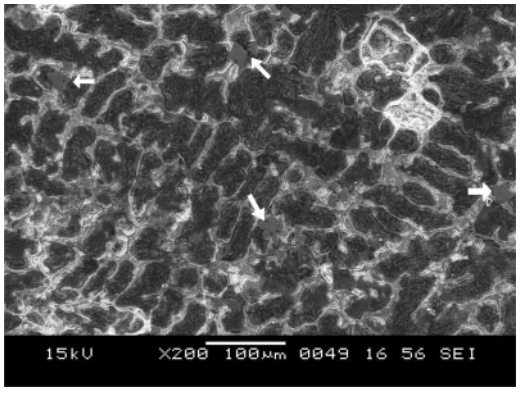

10 Image (SEM) of modified ZA8 alloy solidified in fire-clay crucible

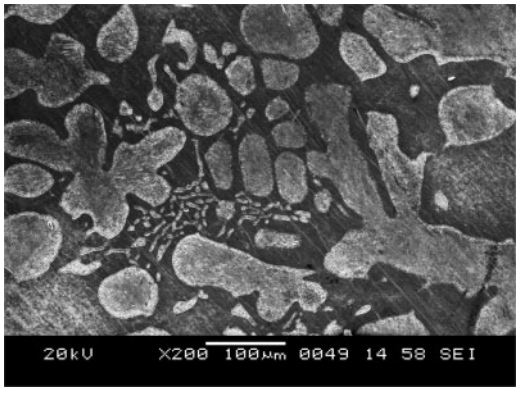

12 Image (SEM) of modified ZA8 alloy solidified against HDS chill

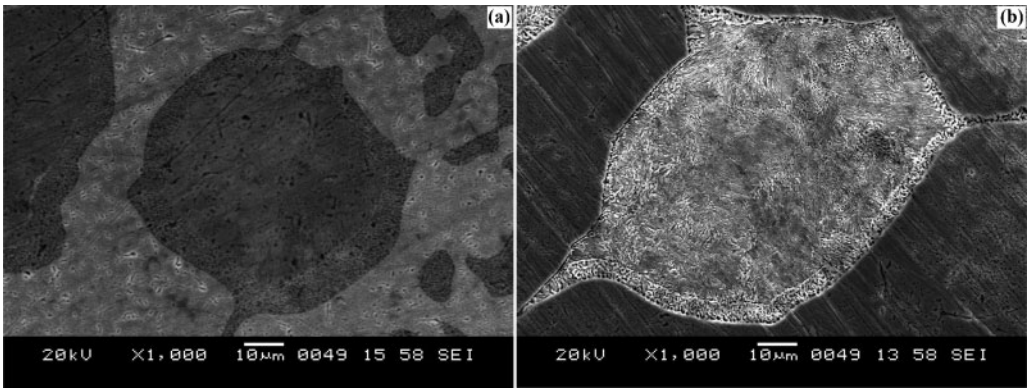

13 Image (SEM) at higher magnification of β phase of *a* unmodified and *b* modified ZA8 alloy solidified against HDS chill

Conclusions

Based on the results and discussion, the following conclusions were drawn.

1. The addition of Mn to ZA8 alloy has a significant effect on thermal analysis parameters. The addition of Mn results in an increase in liquidus temperature and decreases in eutectic and eutectoid temperatures. A liquidus arrest of ~31 s and a small degree of undercooling of 0·12°C at the start of eutectic and eutectic depression of ~9°C were found with chemically modified ZA8 alloy.

2. Chilling of unmodified alloy showed that the liquidus and eutectic start temperatures of the casting remained nearly the same, whereas eutectoid transformation occurred at a higher temperature.

3. Chilling of modified alloy showed decreased liquidus temperature, avoiding the formation/nucleation of intermetallic during solidification. Further, eutectoid transformation was clearly observed and was not seen when unmodified casting was solidified against chill.

4. The addition of Mn decreased the heat of solidification and lowered wettability of ZA8 alloy.

5. Mn modified alloys showed lower peak heat flux as compared to unmodified alloys for all chills.

6. The addition of Mn results in increased volume fraction of dendritic phase and decreased amount of eutectic phase compared to unmodified ZA8 alloy. Further, the modified ZA8 alloy showed the presence of irregularly shaped $MnAl_6$ intermetallic compound.

7. Chilling of the casting results in as cast dendrite morphology transforming to nearly rounded/globular shape with increased volume fraction of eutectic. Chilling with chemical modification enhances the eutectoid transformation and results in enhanced decomposition of β phase.

Acknowledgement

The authors gratefully acknowledge the financial support provided by the Defense Research Development Organization (DRDO), Government of India, New Delhi, under an R&D project.

References

1. E. Gervais, H. Levert and M. Bess: *Trans. AFS*, 1980, **88**, 183–194.
2. 'Alloy data', 'NADCA product specification standards for die castings', Section 3, 2003.
3. http://www.nshoremfg.com/ZINC_CASTING_ALLOYS.pdf (accessed on 22 November 2011).
4. Y. Long, Y.-Y. Li, D.-T. Zhang, C. Qiu and W.-P. Chen: *Trans. Nonferrous Met. Soc. China*, 2002, **12**, 775–779.
5. Y.-Y. Li, Y. Long, W.-P. Chen, D.-T. Zhang and M. Shao: *Trans. Nonferrous Met. Soc. China*, 2002, **12**, 1091–1094.
6. C. Dominguez, M. V. Moreno Lopez and D. Rios-Jara: *J. Mater. Sci.*, 2002, **37**, 5123–5127.
7. Y. H. Zhu, W. B. Lee and S. To: *J. Mater. Sci.*, 2003, **38**, 1945–1952.
8. B. K. Prasad: *Wear*, 2000, **240**, 100–112.
9. T. Savaskan and O. Bican: *Mater. Sci. Eng. A*, 2005, **A404**, 259–269.
10. A. Turk, M. Durman and E. S. Kayali: *J. Mater. Sci.*, 2007, **42**, 8298–8305.
11. Seenappa and K. V. Sharma: *Int. J. Eng. Sci. Technol.*, 2011, **3**, 1783–1789.
12. B. Krupinska, L. A. Dobrzanski, Z. M. Rdzawski and K. Labisz: *Arch. Mater. Sci. Eng.*, 2010, **43**, 13–20.
13. B. Krupinska, Z. M. Rdzawski and K. Labisz: *AMM*, 2011, **46**, 154–160.
14. R. Mojaver and H. R. Shahverdi: *Wear*, 2011, **271**, 2899–2908.
15. 'ZA8 hot chamber die casting guidelines', Eastern Alloys, Inc, http://www.eazall.com/casehistories.aspx (accessed on 22 November 2011).
16. 'Alloy phase diagrams', in 'ASM handbook', (ed. H. Baker and H. Okamoto), Vol. 3; 1992, Materials Park, OH, ASM International.
17. G. V. Raynor and D. W. Wakeman: *Proc. R. Soc. London A: Math. Phys. Sci.*, 1947, **190**, 82–101.
18. G. Ramesh and K. N. Prabhu: 'Heat transfer at the casting/chill interface during solidification of commercially pure Zn and Zn base alloy (ZA8)', *Int. J. Cast Met. Res.*, 2012, **25**, (3), 160-164.
19. H. V. Guthy: 'Evolution of the eutectic microstructure in chemically modified and unmodified aluminum silicon alloys', Master's dissertation, Worcester Polytechnic Institute, Worcester, MA, USA, 2002.